DESIGN AND CONTROL OF A FLYWHEEL INVERTED PENDULUM SYSTEM

José R. C. Vasconcelos*, Elizabeth M. Astorga González†, Pedro M. G. del Foyo*

*Departamento de Engenharia Mecânica, Universidade Federal de Pernambuco
Av. Acadêmico Helio Ramos s/n, CEP 50670-901
Recife/PE, Brasil

†Departamento de Ingeniería Informática, Universidad de Oriente
Santiago de Cuba, CP 90400, Cuba

Emails: roberto.canuto@hotmail.com, eastorga@uo.edu.cu, pedro.foyo@ufpe.br

Abstract— The paper presents an approach to obtain the transfer function of a Flywheel Inverted Pendulum (FIP) prototype when only parameters related to the static mechanical structure are known (mass and pendulum length). The proposed approach combine analytical and experimental techniques, the former conducted over the non-inverted version, since the FIP has an unstable nature. The state space representation is also determined and a digital PID controller is implemented to compute the DC motor voltage required to balance the FIP. A Matlab simulation and experiments with the built prototype have been carried out to validate the effectiveness of the proposed method.

Keywords— flywheel inverted pendulum, experimental identification, PID controller

Resumo— O artigo apresenta uma abordagem para obter a função de transferência de um protótipo de Pêndulo Invertido atuado através de um Volante de Reação (PIVR) quando somente os parâmetros relacionados à estrutura mecânica estática são conhecidos (massa e comprimento do pêndulo). A abordagem proposta combina técnicas analíticas e experimentais, a última realizada sobre a versão não invertida, uma vez que o PIVR tem uma natureza instável. A representação do espaço do estado também é determinada e um controlador PID digital é implementado para calcular a tensão do motor CC necessária para equilibrar o PIVR. Simulações usando Matlab e experiências usando o protótipo construído foram realizadas para validar a eficácia do método proposto.

Palavras-chave— Volante de reação, pêndulo invertido, identificação experimental, Controlador PID

1 Introduction

Flywheel Inverted Pendulum (FIP) is a type of under-actuated mechanical system, which consists of an inverted pendulum and a rotating inertia wheel. Inverted pendulum is a control system with the feature of high order, multi-variable, non-linearity and naturally unstable (Ruan and Wang, 2010). The main objective of an FIP system is to keep the pendulum balance based on the reaction torque following the Newton third law. The reaction torque is produced by the flywheel, which is driven by a DC motor.

As other inverted pendulum models such as cart-pole, acrobat, pendubot, FIP is one of the most favorite nonlinear system for testing and verifying control algorithms (Nguyen and Huynh, 2016). This class of mechanical system has received a lot of interest as they appear in many practical applications like the balance in unicycle vehicles (Jin et al., 2016) or even for moving devices in an environment in which the mechanical and electronic parts can not be exposed (Gajamohan et al., 2013).

There are already many applications based on convencional control methods (Olivares and Albertos, 2013; Nguyen and Huynh, 2016), space-state based methods (Block et al., 2007), fuzzy control method (Ruan and Wang, 2010) among others.

Generally, the system model is obtained through rigorous procedures based on physics principles and then linearized. That was the case for all those works cited here. However they consider all model parameters as knowns even those depending on the DC motor characteristics. In most cases it is very difficult to create an accurate analytical model due to the system complexity and lack of information. In those cases, an approach that combines analytical modeling and parameter estimation using plant data must be applied.

Since the FIP system is naturally unstable an stable version of the FIP, the Flywheel Pendulum, must be considered for the experimental identification approach.

The main objective of this paper is to obtain a transfer function which accurately represent the behavior of the FIP. Also, an state space model with an state vector composed by standard directed measured variables[1] need to be obtained in order to apply state space control methods in future works. It is also presented a conventional control algorithm based on PID digital controller to stabilize the FIP system.

[1]The standard state space vector is composed by the pendulum angular position, the pendulum angular velocity and the flywheel angular velocity.

2 Mathematical Model

The DC motor modeling does not depend on the pendulum position. The dynamics of the DC motor can be obtained using the Kirchoff's law and the Newton's second law. Fig. 1 shows the equivalent electric circuit and the free-body diagram of the rotor.

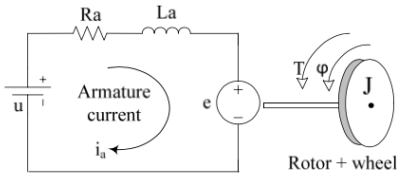

Figure 1: DC motor equivalent model.

$$L_a\frac{di_a}{dt} + R_a i_a + K_v\frac{d\varphi}{dt} = u \quad (1)$$

$$J\frac{d^2\varphi}{dt^2} + b_m\frac{d\varphi}{dt} = K_t i_a \quad (2)$$

Neglecting the armature inductance (L_a), (1) and (2) can be transformed in (3):

$$J\frac{d^2\varphi}{dt^2} + \left(b_m + \frac{K_v K_t}{R_a}\right)\frac{d\varphi}{dt} = \frac{K_t}{R_a}u \quad (3)$$

Since the parameters K_v, K_t, b_m, J and R_a are constants, (3) can be rewritten as:

$$\frac{d^2\varphi}{dt^2} + K_2\frac{d\varphi}{dt} = K_1 u \quad (4)$$

where K_1 and K_2 are constants to be estimated from plant experiments.

The mechanical part of the FIP system consists of a pendulum and a flywheel as shown in Fig. 2

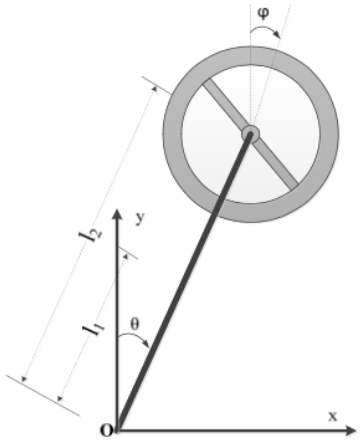

Figure 2: Flywheel Inverted Pendulum mechanical model.

As showed in (Nguyen and Huynh, 2016), considering all torques applied to the pendulum, (5) describes the pendulum movement:

$$J\frac{d^2\theta}{dt^2} + b\frac{d\theta}{dt} - (m_1 l_1 + m_2 l_2)g\sin\theta = -J_2\frac{d^2\varphi}{dt^2} \quad (5)$$

where $J = m_1 l_1^2 + m_2 l_2^2 + J_1 + J_2$. J_1 and J_2 are respectively the pendulum moment of inertia and the wheel moment of inertia.

When considered the Flywheel Pendulum in its not inverted position, angle θ must be replaced with $180° + \theta$. Linearizing (5) for that angle[2] (6) was obtained:

$$J\frac{d^2\theta}{dt^2} + b\frac{d\theta}{dt} + (m_1 l_1 + m_2 l_2)g\theta = -J_2\frac{d^2\varphi}{dt^2} \quad (6)$$

Applying Laplace Transform considering null initial conditions in (6) the Transfer Function (TF) $\frac{\Theta(s)}{\Phi(s)}$ was obtained

$$\frac{\Theta(s)}{\Phi(s)} = \frac{-J_2 s^2}{Js^2 + bs + mlg} \quad (7)$$

where $ml = m_1 l_1 + m_2 l_2$

Applying Laplace Transform considering null initial conditions in (4) the TF $\frac{\Phi(s)}{U(s)}$ was obtained

$$\frac{\Phi(s)}{U(s)} = \frac{K_1}{s(s + K_2)} \quad (8)$$

The TF $\frac{\Theta(s)}{U(s)}$ describe the relationship between the pendulum angle position and the voltage applied to the DC motor.

$$\frac{\Theta(s)}{U(s)} = \frac{-J_2 K_1 s^2}{s(s + K_2)(Js^2 + bs + mlg)} \quad (9)$$

$$= \frac{-\frac{J_2 K_1}{J}s^2}{s^4 + (K_2 + \frac{b}{J})s^3 + \frac{(mlg + K_2 b)}{J}s^2 + \frac{mlgK_2}{J}s} \quad (10)$$

3 FIP system construction

The FIP prototype was built in PLA, using a 3D printing device for the construction of mechanical parts. The design was made using **Solidworks** and it is shown in Fig. 3.

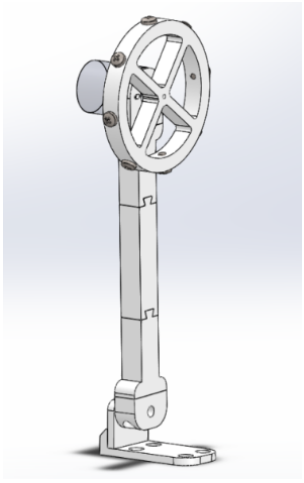

Figure 3: FIP prototype mechanical design.

[2] $\sin(180 + \theta) \approx -\theta$ when -15° $\leq \theta \leq$ 15°

The FIP system is composed of an angular position sensor, which was implemented using a 10 KΩ potentiometer. A DC motor model *AK360/PL 12-12500* is driven by a H-Bridge **L298N** using a 12 V power supply. The hardware controller was based on the **Arduino Nano** platform. Full hardware controller is shown in Fig. 4.

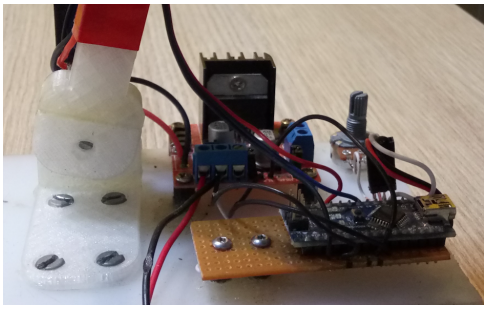

Figure 4: Flywheel Inverted Pendulum hardware controller.

4 Experimental identification

The experiments were conducted using a 10 ms sampling time (100 Hz). The first experiment conducted used a step signal in order to identify the system natural frequency. Using data from that experiment, 5 Pseudo Random Binary Signals (PRBS) were generated, using *idinput* command available in **Matlab** software according to parameters established in (Ljung, 1999)

The plant data obtained using those 5 PRBS as input are shown in Fig. 5

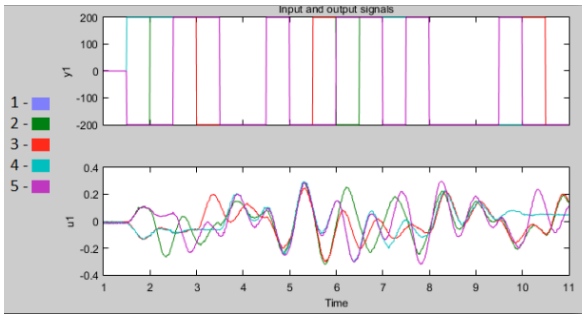

Figure 5: Data from five experiments on **Matlab System Identification Toolbox** user interface.

For those experiments, the input signal is the DC motor voltage and the output signal is the pendulum angular position in rad, precomputed from the potentiometer voltage. Then, the constant used to convert voltage to angle was already included in the TF to be determined. Model parameters estimation was conducted using the **Matlab** System Identification Toolbox (Ljung, 1992).

Equation (10) shows the TF desired structure, which is a two zeros, 4 poles with no delay. Using **Matlab** identification toolbox function *Estimate* → *Transfer Function Models*, a TF was obtained with 4 poles and 2 zeros. The model obtained achieved a 89.19 % precision.

$$G_1(s) = \frac{-0.02882s^2 - 0.001487s + 0.006707}{s^4 + 2.467s^3 + 76.05s^2 + 46.67s + 1.1 \times 10^{-10}}$$

The $G_1(s)$ transfer function was adapted to fit the desired model structure leading to a 84.77 % precision.

$$G_2(s) = \frac{-0.03s^2}{s^4 + 2.467s^3 + 76.05s^2 + 46.67s} \quad (11)$$

Table 1 shows the precision obtained using different experiment data.

Table 1: Model precision for each experiment (%)

TF	Exp1	Exp2	Exp3	Exp4	Exp5
$G_1(s)$	89.19	82.65	80.97	81.35	85.1
$G_2(s)$	84.77	83.1	79.09	80.45	87.12

Even when model precision was better for $G_1(s)$ the step response fails to follow the real behavior of the FIP system while model $G_2(s)$ presented the correct behavior.

5 Obtaining the FIP Transfer Function

The FIP transfer function can be obtained from G2 transfer function. Note that FIP must operate around 0° while the stable version operate around 180°. The linearization of eq. 5 will follow the next equation:

$$J\frac{d^2\theta}{dt^2} + b\frac{d\theta}{dt} - (m_1l_1 + m_2l_2)g\theta = -J_2\frac{d^2\varphi}{dt^2} \quad (12)$$

Considering equations 8 and 12, the TF of the FIP is:

$$\frac{\Theta(s)}{U(s)} = \frac{-\frac{J_2K_1}{J}s^2}{s^4 + (K_2 + \frac{b}{J})s^3 + \frac{(K_2b - mlg)}{J}s^2 - \frac{mlgK_2}{J}s}$$

Note that terms s^4 and s^3 remains the same and term s will be the same but negative. Coefficient for term s^2 must be determined.

Since parameters m_1, l_1, m_2, l_2 can be easily obtained from the FIP design and g is known there is a system of algebraic equations of size three. Table 2 shows the FIP known parameters.

Table 2: FIP known parameters

Symbol	Description	Value
m_1	pendulum mass	0.015 Kg
m_2	motor and wheel mass	0.0995 Kg
l_1	pendulum mass center	0.13 m
l_2	pendulum length	0.169 m

$$
\begin{aligned}
K_2 + \frac{b}{J} &= 2.467 \\
\frac{(K_2 b + 0.1839)}{J} &= 76.05 \\
\frac{0.1839 K_2}{J} &= 46.67
\end{aligned}
$$

The parameters value obtained were $K_2 = 0.6342$, $b = 0.0046$ and $J = 0.0025\,\mathrm{Kg/m^2}$. Solution for J comes from a third order polynomial equation with one real solution (0.0025) and two discarded complex solutions.

The TF of the FIP system is:

$$
\frac{\Theta(s)}{U(s)} = \frac{-0.03 s^2}{s^4 + 2.467 s^3 - 72.4 s^2 - 46.67 s} \tag{13}
$$

The FIP system's negative gain means that clockwise rotation in DC motor, obtained applying a negative voltage, increases the pendulum angular position, while counter-clockwise rotation in DC motor, obtained applying a positive voltage, decreases the pendulum angular position.

5.1 Validating the FIP Transfer Function

The homogeneous version of (6) can be used to determine some system parameters such as the system frequency ω.

$$
\frac{d^2\theta}{dt^2} + \frac{b}{J}\frac{d\theta}{dt} + \frac{mlg}{J}\theta = 0 \tag{14}
$$

Since the system behavior is underdamped the (14) solution has the form:

$$
\theta(t) = e^{\sigma t}(c_1 \cos \omega t + c_2 \sin \omega t) \tag{15}
$$

where $\sigma = -\frac{b}{2J}$ and $\omega = \frac{\sqrt{b^2 - 4Jmlg}}{2J}$

Note that ω is the system damping frequency and can be validated trough the system impulse response. The $G2$ impulse response obtained using **Matlab** is shown in Fig. 6.

Frequency of $G2$ was obtained by:

$$
\frac{2\pi}{\omega_d} = 0.733\,\mathrm{s} \Rightarrow \omega_d = 8.57\,\mathrm{rad/s} \Rightarrow f_d = 1.364\,\mathrm{Hz}
$$

The frequency obtained analytically from FIP parameters was $\omega_d = 8.5277\,\mathrm{rad/s}$ which confirm data obtained by experimental identification.

The frequency spectrum of potentiometer signal in experiment 5 (Exp5) is shown in Fig. 7

The frequency spectrum shows two important things:

- There are 4 dominant frequencies, the more important of them is the damping frequency of mechanical system $f_d = 1.401\,\mathrm{Hz} \approx 1.364\,\mathrm{Hz}$;

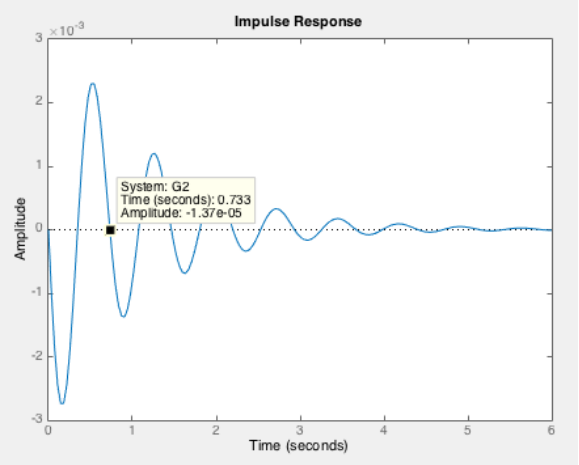

Figure 6: Impulse response of TF $G2$ obtained with **Matlab**.

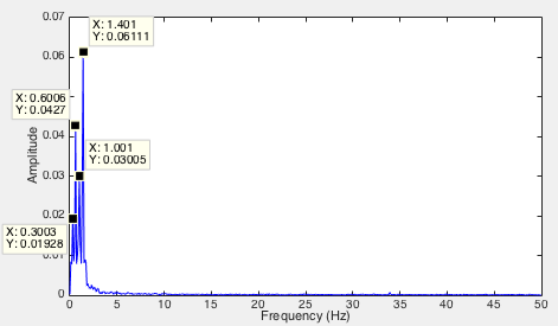

Figure 7: Frequency spectrum of pendulum angular position in experiment 5.

- There are no significant information above 5 Hz frequency. According to Nyquist-Shannon Theorem, a sampling rate of 10 Hz (two times 5 Hz) will ensure no information losses when sampling the pendulum angular position.

6 The FIP State Space Model

To obtain the FIP state space model parameters J_2, and K_1 are necessary. Considering the total moment of inertia J and assuming that the wheel moment of inertia (J_2) is many times greater than the pendulum moment of inertia J_1,[3] so J_2 can be computed by:

$$
\begin{aligned}
J_1 + J_2 &= J - (m_1 l_1^2 + m_2 l_2^2) \\
J_1 + J_2 &= 0.000\,595\,\mathrm{Kg/m^2} \\
J_2 &\approx 0.9(J_1 + J_2) = 0.000\,536\,\mathrm{Kg/m^2}
\end{aligned}
$$

From the FIP model (11) and (12), the parameter K_1 can be estimated.

$$
-\frac{J_2 K_1}{J} = -0.03 \Rightarrow K_1 = \frac{0.03J}{J_2} = 0.14
$$

[3] It is assumed here that J_2 is 90% of the total moment of inertia J

The FIP state space model is given as follow:

$$\begin{bmatrix}\dot{\theta}\\ \ddot{\theta}\\ \dot{\phi}\\ \ddot{\phi}\end{bmatrix} = \begin{bmatrix}0 & 1 & 0 & 0\\ \frac{mlg}{J} & -\frac{b}{J} & 0 & \frac{J_2K_2}{J}\\ 0 & 0 & 0 & 1\\ 0 & 0 & 0 & -K_2\end{bmatrix}\begin{bmatrix}\theta\\ \dot{\theta}\\ \phi\\ \dot{\phi}\end{bmatrix} + \begin{bmatrix}0\\ -\frac{J_2K_1}{J}\\ 0\\ K_1\end{bmatrix} u$$

Substituting the FIP parameters the system representation was obtained:

$$\begin{bmatrix}\dot{\theta}\\ \ddot{\theta}\\ \dot{\phi}\\ \ddot{\phi}\end{bmatrix} = \underbrace{\begin{bmatrix}0 & 1 & 0 & 0\\ 73.56 & -1.83 & 0 & 0.13\\ 0 & 0 & 0 & 1\\ 0 & 0 & 0 & -0.63\end{bmatrix}}_{\mathbf{A}}\begin{bmatrix}\theta\\ \dot{\theta}\\ \phi\\ \dot{\phi}\end{bmatrix} + \underbrace{\begin{bmatrix}0\\ -0.03\\ 0\\ 0.14\end{bmatrix}}_{\mathbf{B}} u$$

The eigenvalues of state matrix **A** are $[7.7092\ -9.5420\ 0\ -0.6342]^T$ which correspond with poles in TF in (13).

Note that, the flywheel angular position (ϕ), does not affect any other variable[4]. Thus, if there is not any interest in its evolution, it can be discarded leading to a more simplified state space model as in (Olivares and Albertos, 2013).

$$\begin{bmatrix}\dot{\theta}\\ \ddot{\theta}\\ \ddot{\phi}\end{bmatrix} = \begin{bmatrix}0 & 1 & 0\\ 73.56 & -1.83 & 0.13\\ 0 & 0 & -0.63\end{bmatrix}\begin{bmatrix}\theta\\ \dot{\theta}\\ \dot{\phi}\end{bmatrix} + \begin{bmatrix}0\\ -0.03\\ 0.14\end{bmatrix} u$$

7 Control Strategy

In this paper, the control strategy only concern was the system stabilization. In doing so, there was necessary to deal with some issues like noise generated by the potentiometer, saturation and dead zone in DC motor behavior.

The controllability of FIP can be established by the controllability matrix:

$$\begin{aligned} Co &= [B \quad AB \quad A^2B \quad A^3B] \\ &= \begin{bmatrix}0 & -0.0300 & 0.0740 & -2.3549\\ -0.03 & 0.0740 & -2.3549 & 9.7687\\ 0 & 0.1400 & -0.0888 & 0.0563\\ 0.14 & -0.0888 & 0.0563 & -0.0357\end{bmatrix}\end{aligned}$$

Since the rank of Co matrix is 4, it corresponds to the size of the state space vector $[\theta\ \dot{\theta}\ \phi\ \dot{\phi}]^T$. Thus FIP is a completely controllable system.

The ideia was to implement a PID controller with a lowpass filter in the derivative action and anti-windup feature. To deal with the noise generated by the potentiometer it was decided to turn off the derivative action when the pendulum angular position reached certain balance range.

It was also used a positive feedback loop in order to deal with positive gain for PID controller. The control architecture is shown in Fig. 8

The K gain was used to convert from rad to degrees.

[4]Third column of the states matrix **A** is null

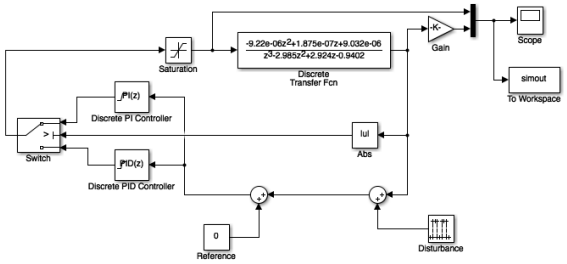

Figure 8: Control strategy for balancing FIP.

7.1 Choosing an appropriate sampling time

Since a digital controller will be used, the sampling time for the control loop must be determined and the plant must be discretized for the chosen sampling time. Even when the Nyquist-Shannon theorem is satisfied, for control purposes, such sampling rate is not enough to satisfy the system performance requirements.

Besides the desired behavior of the closed-loop response, other requisites must be considered like processor time consumption, which its related to the power consumption. Such requirement is an important feature when dealing with embedded systems.

The sampling rate was chosen being as slow as possible, but fast enough to allow to achieve balance, avoiding to reach the controller action saturation limits.

The relevant higher frequency was obtained from Fig. 7, which was about 2 Hz. A sampling rate of ten times that frequency was considered in order to achieve a system performance similar to the continuous transfer function.

Using a 20 Hz sampling rate (a sample time $T_s = 0.05$ s), the discrete TF was obtained. The **Matlab** Graphical Controller Design Toolbox was then used to tune a PID controller. Even when the system became stable, the controller gain was so high that the control action blowup the saturation limits resulting in an unstable closed-loop response, when saturation effects were considered.

The procedure was repeated for a sampling rate of 25 Hz ($T_s = 0.04$ s) with similar results and then with a sampling rate of 40 Hz ($T_s = 0.025$ s) when the stability condition was achieved even considering the saturation of the control action.

The discrete-time transfer function was:

$$G(z) = \frac{-9.22 \times 10^{-6}z^2 + 1.87 \times 10^{-7}z + 9.03 \times 10^{-6}}{z^3 - 2.985z^2 + 2.924z - 0.9402}$$

7.2 Simulation results

Simulations results for the controlled FIP when subject to a disturbance impulse with 0.15 rad amplitude and 0.5 s duration are shown in Fig. 9.

The FIP response in Fig. 9 was obtained for PID controller parameters (Kp=6500,

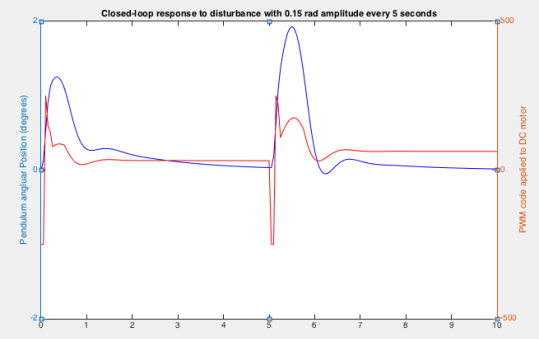

Figure 9: Simulation results of controller FIP.

Ki=3500 and Kd=700) and PI controller parameters (Kp=5000, Ki=2200). The PI controller was activated when $-1.15\,^\circ \leq \theta \leq 1.15\,^\circ$.

8 Experimental Results

The control strategy shown in Fig. 8 was implemented in the laboratory prototype. The experimental results obtained using the same parameters in simulation are shown in Fig. 10.

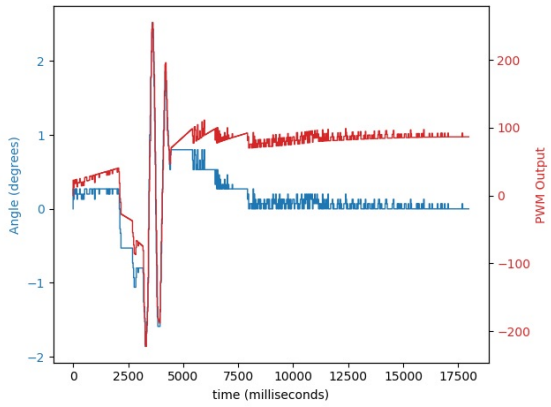

Figure 10: Experimental results of controller FIP.

In this experiment the disturbance was applied by a slight tapping on the pendulum rod in order to remove it from the equilibrium position.

Other experiments were conducted using sampling rates of 20 Hz and 25 Hz but the system could not remain in balance for more than 5 seconds even when no disturbance was applied.

9 Conclusion

The approach here proposed allows to determine the FIP transfer function even when dealing with a system that is naturally unstable and not all parameters were known or easily determined.

Despite the simplicity of the control strategy, the FIP was successfully stabilized using the exact tuning obtained in simulation which confirm the obtained transfer function validity. The adequate sample rate was also determined based on simulations. Several implementations of the controller using faster sampling rates fails like predicted by simulation.

Acknowledgements

The authors wants to thank Prof. Felix C. G. Santos for his assistance with the english translation and comments on an earlier version of the manuscript.

References

Block, D., Ãnström, K. J. and Spong, M. W. (2007). *The reaction wheel pendulum*, Vol. 1 of *Synthesis Lectures on Control and Mechatronics*, Morgan & Claypool, pp. 1–105.

Gajamohan, M., Muehlebach, M., Widmer, T. and Andrea, R. D. (2013). The cubli: A reaction wheel based 3d inverted pendulum, *European Control Conference (ECC)*, pp. 268–274.

Jin, H., Wang, T., Yu, F., Zhu, Y., Zhao, J. and Lee, J. (2016). Unicycle robot stabilized by the effect of gyroscopic precession and its control realization based on centrifugal force compensation, *IEEE/ASME TRANSACTIONS ON MECHATRONICS* **21**(8): 2737–2745.

Ljung, L. (1992). *System Identification Toolbox*, The Mathworks, Inc.

Ljung, L. (ed.) (1999). *System Identification: Theory for the User*, 2nd edn, Prentice Hall PTR, Upper Saddle River, NJ, USA.

Nguyen, T.-S. and Huynh, T.-H. (2016). Study on a two-loop control architecture to balance an inertia wheel pendulum, *3rd National Foundation for Science and Technology Development Conference on Information and Computer Science (NICS)*, IEEE.org, pp. 29–33.

Olivares, M. and Albertos, P. (2013). On the linear control of underactuated systems: the flywheel inverted pendulum, *10th IEEE International Conference on Control and Automation (ICCA)*, IEEE.org, Hangzhou, China, June 12-14,, pp. 27–32.

Ruan, X. and Wang, Y. (2010). The modelling and control of flywheel inverted pendulum system, *3rd IEEE International Conference on Computer Science and Information Technology*, IEEE.org, Chengdu, China.